ACS OMEGA

Open Access

http://pubs.acs.org/journal/acsodf

Article

Reinvigorating Photo-Activated R-Alkoxysilanes Containing 2-Nitrobenzyl Protecting Groups as Stable Precursors for Photo-Driven Si−O Bond Formation in Polymerization and Surface Modification

Mahmud R. Rashed, Cory B. Sims, Shahrea Mahbub, Nai-hsuan Hu, Ashley N. Greene, Herenia Espitia Armenta, Ryan A. Iarussi, and Joseph C. Furgal*

Cite This: *ACS Omega* 2024, 9, 40650−40664

Read Online

ACCESS | Metrics & More | Article Recommendations | Supporting Information

ABSTRACT: This study aimed to revitalize silicon-based sol−gel chemistry methodologies utilizing photoprotected R-alkoxysilanes to control the synthesis of unique silicon-based materials. We have investigated the synthesis, characterization, light-induced deprotection, and subsequent polymerization/surface functionalization through the use of 2-nitrobenzyloxy-based photoremovable protecting groups (PPGs) as alkoxy reactive groups on ethyl and phenyl $(R_x\text{-(alkoxy)}_y$ silanes, with $x = 0-3$ and $y = 1-3$). The photochemical dynamics, relative efficiencies, and kinetics of the novel alkoxysilane-based PPGs were thoroughly investigated using UV light irradiation by NMR and UV/vis methods. We then explored the tin-catalyzed coupling of photodeprotected products (R_x-silanols) to form polymers/oligomers. We have found that photoenabled removal of PPGs and conversion to silanols from all silane systems studied is achieved. Furthermore, these deprotected species are polymerizable into siloxanes and effectively used as light-controlled surface modifiers with masking techniques of which proof-of-concept examples are given, enabling promising application as photolithographic reagents.

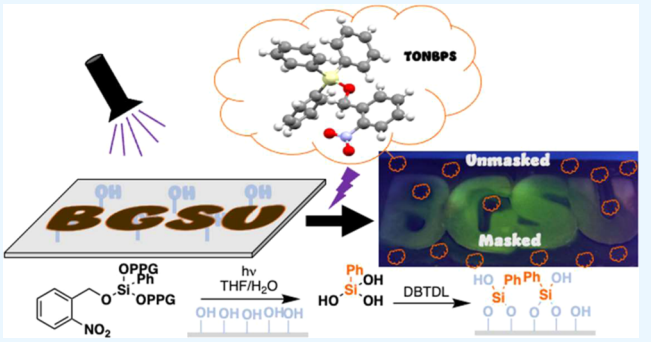

INTRODUCTION

R-alkoxysilanes are the monomer workhorses of silicon-based sol−gel chemistry and are used as the building blocks for various materials from silica to silicone.[1−3] However, uncontrolled hydrolysis, premature condensation, and overall polymerization control have plagued the sol−gel and siloxane communities since their inception, giving significant sol−gel derived byproducts that can be difficult or impossible to remove and exhibit low surface functionalization control.[4] Furthermore, purification difficulties abound for many alkoxysilanes with large and bulky R-groups, as they cannot be easily distilled.[6,7] These reasons have, therefore, limited the development and use of silanes for controlled and unique polymerization reactions.

The stability of R-alkoxysilanes is often improved by using bulkier alkoxy groups such as iso-propoxy and tert-butoxy instead of smaller more common methoxy/ethoxy.[8−11] This method is quite effective at limiting premature hydrolysis of reagents, however, the subsequent polymerization reaction rates become extremely sluggish and uncontrolled because accessibility to the silicon core is much more hindered.[12] Another strategy has been to use groups such as benzyl groups (similar sterics to iso-propoxy) which can be removed by reduction methods with Pd/C or Pt/C and H_2 without the need for hydrolysis conditions.[13] This method can lead to contamination with activated carbon, which is difficult to remove from synthesized materials. These methods tend to fall short in their own ways, leaving the door open for other techniques.

Photochemical release groups are very useful in organic synthesis, protecting against undesired reactions until the preferred time. One of the major advantages of these techniques is the use of light for the activation of a chemical compound in a specific region and time (i.e., spatial and temporal control).[14,15] Photoremovable protecting groups or photocages (PPG) were first developed by Barltrop and Schofield in 1962,[16,17] where they synthesized glycine-carbamate by using 254 nm UV light to photorelease a benzyloxy photoreactive group from benzyloxy-carbonyl-

Received: May 22, 2024
Revised: September 3, 2024
Accepted: September 11, 2024
Published: September 17, 2024

Scheme 1. Photocaging of Alkoxysilane Using the ONB Group[26a]

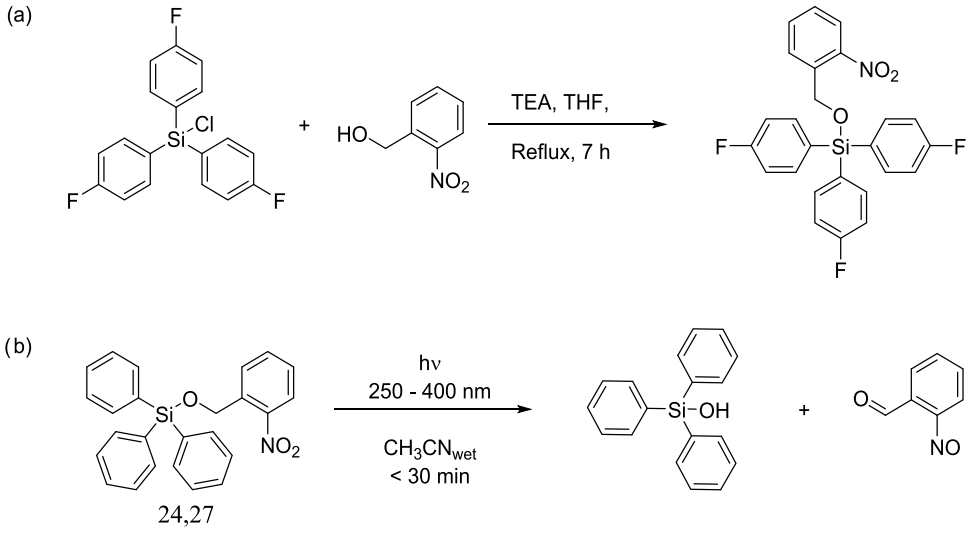

[a](a) Synthesis of (2-nitrobenzyloxy)tri-*p*-fluorophenylsilane.[26] (b) Photodecomposition of (2-nitrobenzyloxy)triphenylsilane in wet acetonitrile under UV irradiation.[24,27]

glycine. PPG applications go well beyond releasing simple organic compounds and apply to pharmaceutical reagents, biochemical molecules, photolithography, and more.[14,18−20] Barltrop et al. expanded to 2-nitrobenzyloxy (**ONB**) PPG in 1970, establishing it as the most used workhorse in photocaging.[14,16,21] Since that time, several protecting groups have been discovered and implemented in a variety of chemical developments, but 2-nitrobenzyl groups remain popular due to their low cost and efficiency. These groups are commonly used for the protection of alcohols to form 2-nitrobenzylmethyl ethers, which upon photoirradiation in aqueous solutions lead to 2-nitrosobenzaldehydes (**NsBAlds**) as a byproduct and free alcohols.[22,23] In our project, 2-nitrobenzyl alcohol was utilized due to its relatively low cost, ease of attachment to R-chlorosilanes, and extensive study of its photodynamic properties and interactions.

Using bulky photodeprotection groups that enable light to be used as a nonchemical trigger is one way to overcome some of the challenges of alkoxysilane chemistry. There are a limited number of previous reports on alkoxysilane photoprotecting groups from the 1980's[24−27] in which the development of 2-nitrobenzyloxy photoprotections of $(alkoxy)_{n=1-3}(R)_{m=1-3}$ silanes was the primary goal.[24] Though the initial motivation was to develop photocurable siloxanes,[24] much of this literature has focused on their use as cocatalysts for the polymerization of epoxy resins.[25−28]

The methods by which photoprotected R-alkoxysilanes are synthesized and phototriggered are straightforward. An example by Yamamuro et al. is shown in Scheme 1a. Irradiation of the product in this scheme using a mercury lamp showed that silanols were formed and were able to be coupled, although many details such as reaction efficiency and kinetics are not available in this previous literature. For most of the examples, slightly electron-withdrawing R-group substituents resulted in better photoreleasing efficiencies of the 2-nitrobenzyl alcohol (i.e., chloro or fluorophenyls), likely due to weakening of the Si−O bond.[26] Work by Hayase et al. showed that photodecomposition of (2-nitrobenzyloxy)triphenylsilane (in acetonitrile) irradiated by a high-intensity mercury lamp took ∼30 min to reach full conversion to silanol (Scheme 1b).[24,27] They also found that photocurable polydimethylsiloxanes from bis(2-nitrobenzyloxy)dimethylsilane with 6000 cSt viscosities were possible after irradiation in the presence of a silanol condensing catalyst (dibutyltin-dilaurate, **DBTDL**), whereas dimethoxy-dimethylsilane showed no reactivity under these same conditions.[21] From these studies, no extensive investigation of stability, advanced spectroscopic analysis, R-group reactions, or reaction kinetics (PPG or polymerization) was determined. This left an open platform for reinvigorating these types of 2-nitrobenzyloxy-protected alkoxysilanes for modern uses and driving further expansion to other protecting group strategies.

The investigation of synthesis and the fundamental examination of their reactivity for these alkoxysilanes are extended to explore their real-world application in sol−gel-type reactions. Silanes, including chlorosilanes and alkoxysilanes, are used for modifying surfaces. During the process of hydrolysis, the two silanes undergo transformation into silanols in the presence of water. The silane coupling process facilitates the binding of silanols to hydroxy (OH) groups present on the surface of a substrate, resulting in the release of water as a byproduct through condensation. There are many examples of standard acid/base/thermal surface functionalization, and here we give just a few: Jung et al. demonstrated that alkoxysilanes, such as (3-aminopropyl)triethoxysilane (APTES), 1*H*,1*H*,2*H*,2*H*-perfluorodecyltriethoxysilane, and *N*-octyltriethoxysilane, were able to modify the surface of MXene, chosen for its affordability, widespread availability, and various end-groups.[29] Velleman et al. conducted a modification of the porous silicon membrane surface by introducing chlorosilane ((heptadecafluoro-1,1,2,2-tetrahydrodecyl)-dimethylchlorosilane) to induce hydrophobicity and alkoxysilane (*N*-(triethoxysilylpropyl)-*o*-poly(ethylene oxide)-urethane) to induce surface hydrophilicity.[30] Rehman et al.'s investigation included the quick modification of the surface of hydroxyapatite nanorods using aminopropyltriethoxysilane and microwave.[31] The amino groups were then used for modifications with bioactive compounds. Examples can be found in the literature of other types of alkoxysilane R-group protection used to reduce the reactivity of the functional group

https://doi.org/10.1021/acsomega.4c04837
ACS Omega 2024, 9, 40650−40664

Scheme 2. Synthesis of ONBRS Compounds and Subsequent Deprotection Using UV Irradiation to form the Corresponding Siloxane/Surface/Silsesquioxane; List of Compounds, Respective Appearance, and Isolated Yield[a]

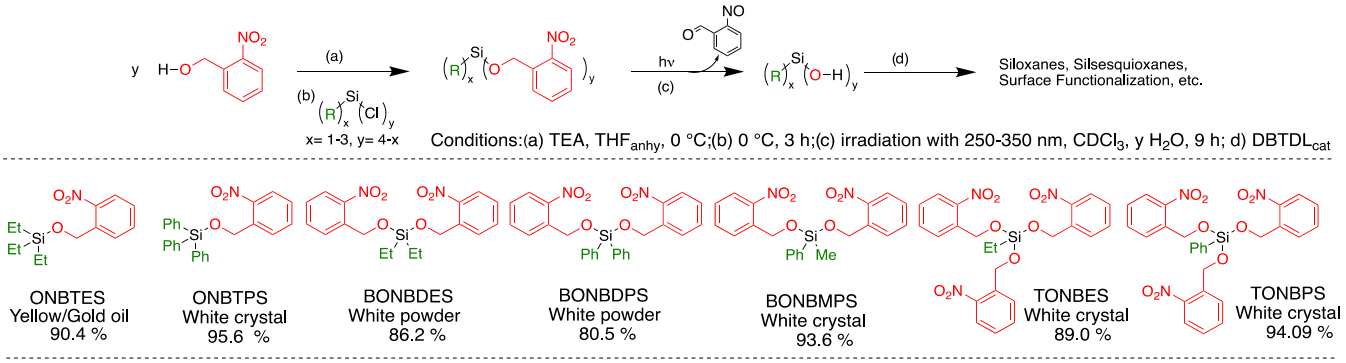

[a]See Table S1 for full compound names.

during attachment to the substrate. Spacing of 3-aminopropyltrimethoxysilane on a surface was achieved by using bulky aromatic protecting groups (trityl and benzyl) to reduce amine interactions during the attachment steps and deprotected by hydrolysis.[32] These methods, however, do not offer a lot of specific control over when and where reactions take place. To overcome this, we turned to photochemical methods. Research by Álvarez et al. demonstrated the photo formation of a carboxylate functionalized silane from 1-(4,5-dimethoxy-2-nitrophenyl)ethyl but-3-enoate after attachment to a surface and irradiation.[33] Similar to this work, Jonas et al. used a 6-nitroveratryloxycarbonyl PPG to protect the amine of 3-aminopropyltriethoxysilane to form photopatterning after hydrolysis.[34] Other examples of surface modification have utilized photoacid generators to selectively initiate the acid-catalyzed siloxane surface condensation.[35] While these methods show promise for surface modification, they come with limitations from the necessity of specific R-groups to the use of acidic components. To circumvent this, a PPG with an easier attachment is ideal.

The use of the **ONB** group photocage offers a multitude of potential applications, notably in surface coatings. Yan et al. utilized the **ONB** group as a cross-linking agent between *N*-hydroxysuccinimidyl and disulfide groups to imbue surface modification of gold-coated proteins. This modification allowed the controlled release of immobilized proteins upon exposure to UV irradiation at a wavelength of 300 nm, while preserving the functioning of the proteins.[36] Chen et al. used an additional methodology in their study, whereby hydrogels were subjected to functionalization with the **ONB** group for the purpose of three-dimensional (3D) printing. Before this, the researchers utilized polylysine and a photomask to selectively change certain surface areas via UV light.[37] These studies used the **ONB** group for either coating a surface with substances that contain the **ONB** group as a cross-linker and releasing the substrate after photolysis, or binding the **ONB** group within a material and later functionalizing the surface using a photomask and UV irradiation.

We have undertaken a fundamental study of the synthesis and characterization of R-alkoxysilanes with 2-nitrobenzyloxy PPGs as a model system (**ONB** group), to selectively trigger their reaction response and limit premature degradation/reactivity, building upon the work of Hayase et al.[27] In this study, we have synthesized a series of 2-nitrobenzyloxy alkoxysilanes (**ONBRS**) with varying functionalities ((alkoxy)$_{n=1-3}$(R)$_{m=1-3}$silanes) and more thoroughly investigated the spatio/temporal-controlled light-driven removal of these protecting groups to trigger sol−gel reactions to make silicon-based compounds and investigated their respective reactions. Furthermore, we have tested the stability of these compounds against various hydrolysis conditions, purification conditions (i.e., column chromatography), their propensity toward forming polymers, and their potential as light-activated surface modifiers.

RESULTS AND DISCUSSION

Herein, we investigate the derivatization of phenyl and ethylchlorosilanes with 2-nitrobenzyloxy (**ONB**) functionalities. These silanes are readily available and have boiling points higher than those of methylchlorosilanes, making them easier to work with. We began with monochloro derivatives such as chlorotriethylsilane (**CTES**) and used substitution with nitrobenzyl alcohol (**NBAlc**) to form 2-nitrobenzyloxytriethylsilanes (**ONBTES**).

Triethylamine (TEA) was used as the base in previous work by Hayase et al.[24] Our initial attempts to form **ONBTES** using their methodology were not successful since clear parameters were not given. Hence, we continued our work to establish a new synthesis strategy. We chose to use sodium hydride (NaH) as the base due to its gaseous removal as H_2. We found that the product could be formed at 0 °C, but it led to lower-than-expected conversions (<75%) after 24 h reaction times. Thus, using NaH proved to be difficult for these reactions and we then revisited the initial methods. Conducting the reaction using TEA as the base at 0 °C instead of the suggested room temperature proved to be highly effective in obtaining **ONBTES** after 3 h with 90+% isolated yield after silica gel column purification. Based on this finding, we proceeded to synthesize the rest of the **ONBRS**s (Scheme 2) using TEA at 0 °C with distilled and dry tetrahydrofuran (THF). Running these reactions under dry nitrogen (N_2) prevented any additional moisture from infiltrating the reactions and leading to side products. Note: Liquid silanes such as **CTES** were added dropwise directly to the mixture of base and **NBAlc**, whereas chlorotriphenylsilane (**CTPS**), a solid, was dissolved in THF before addition. See the Supporting information (SI) for further synthetic details.

We observed that the purification methods of **ONBRS**s depend on their molecular weight and structure. When the M.W. of the alkoxysilane is lower than 424 g/mol (**ONBTES**,

https://doi.org/10.1021/acsomega.4c04837
ACS Omega 2024, 9, 40650−40664

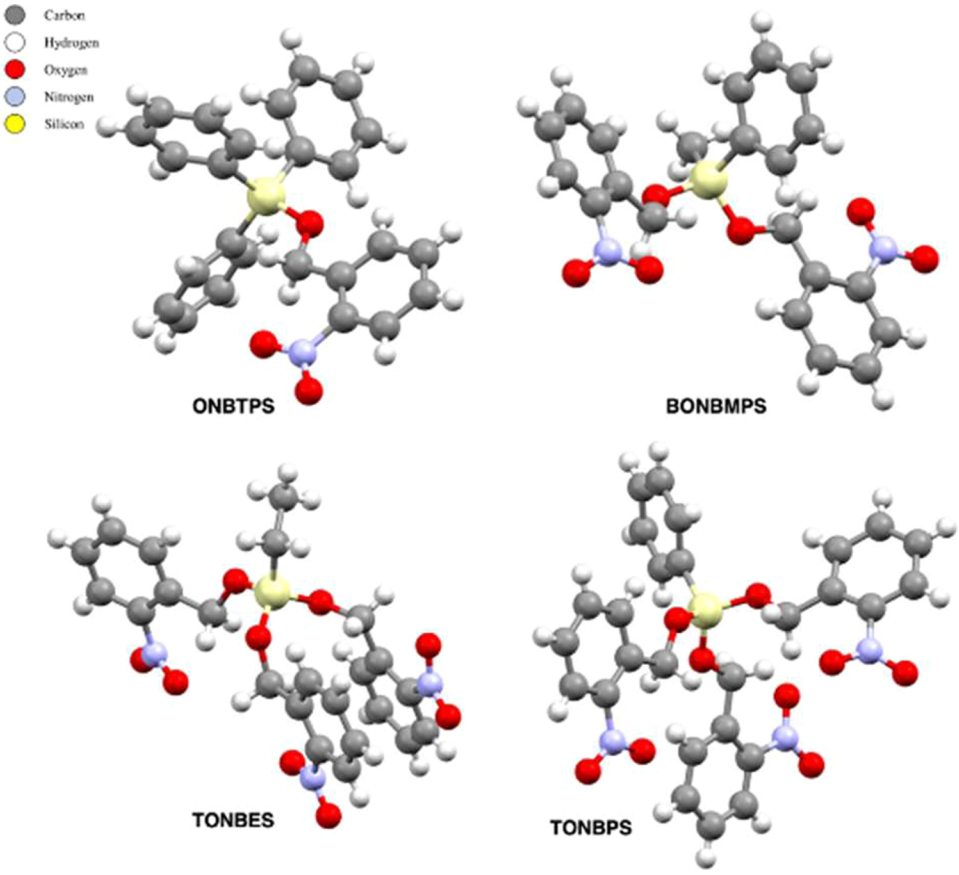

Figure 1. Single Crystal-XRD structures of selected ONBRSs.

ONBTPS, **BONBDES**), silica gel column chromatography using hexanes/dichloromethane (DCM), 1:1, was a better way to purify them rather than using toluene as mentioned in the literature.[27] Alternatively, precipitation using DCM and methanol (1:1) was superior (vs column chromatography) with higher yields in separating the desired product from the crude solution, but only for solid compounds that have a higher propensity to self-crystallize.

Characterizations of all **ONBRSs** were carried out using NMR (^{1}H, ^{13}C, ^{29}Si), high-resolution mass spectrometry (HRMS), thermogravimetric analysis (TGA), Fourier transform infrared (FTIR), and X-ray crystallography (Figures S2−S57 and Tables S2−S4). In ^{1}H NMR, the range in peaks of the benzyloxy methylene group (2H) for all the **ONBRS** compounds was from 5.13 to 5.39 ppm and used for primary confirmation of substitution through a shift from **NBAlc**. For the ethyl-containing compounds, CH_3 (1.02−1.15 ppm) and CH_2 (0.73−0.96 ppm) were observed. The methyl group of **BONBMPS** displayed a distinct peak at 0.59 ppm. The aromatic region (8.15−7.38 ppm) indicated the **ONB**'s phenyl and Si-phenyl (when present) groups. The starting material, 2-nitrobenzyl alcohol, showed 2 peaks at ∼5 ppm, one for the methylene group (2H) and another for the OH group (1H). The presence of a single peak between 5.13 and 5.39 ppm was an indication of the alkoxysilane product formation (i.e., Figure S2). In ^{13}C NMR, the peaks for the methylene group of the alkoxysilanes were at 61.63−62.81 ppm (i.e., Figure S9). The silane ethyl group (CH_2 and CH_3) and the silane methyl group peaks were between 1.96 and 6.74 ppm. Aromatic peaks were in the regions from 124.48 to 146.51 ppm. Each ^{29}Si NMR spectrum showed one silicon peak (Figures S16−S22), reflecting the high purity of the products. Only **ONBTES** had a positive value (+22.08 ppm), whereas the largest negative and most shielded peak was for **TONBPS** at −56.11 ppm. Increasing the number of 2-nitrobenzyloxy rings in the silane caused the silicon peak to move to the negative region as expected due to increased shielding from oxygen.

The composition of each pure **ONBRS** was verified by HRMS, all with $[M + Na]^+$ ions as shown in Figures S23−S29. The TGAs, in air, of all **ONBRS** compounds were reported with $T_{d5\%}$ and ceramic yield (CY) (Table S2 and Figures S30−S36). $T_{d5\%}$ is the mass loss of 5 wt % represented by the initial decomposition temperature, and the CY is the SiO_2 residue yield. $T_{d5\%}$ ranged from 145.13 °C for **ONBTES** to 273.67 °C for **TONBPS**. The lowest CY (0.6%) was obtained for **ONBTES** (volatile), while **TONBPS** showed the highest value (10.1%) due to its nonvolatile nature. The structures of the **ONBRS**s were additionally verified through the utilization of FTIR analysis (Table S3, Figures S37−S43), exhibiting distinct peaks that correspond to the chemical bonds present in these compounds. For instance, the Si−O−C peak was observed within the range of 1000−1100 cm^{-1}, while the benzyl peaks were observed both before and after 3000 cm^{-1}, representing aliphatic and aromatic C−H bonds, respectively. Lastly, the nitro group is visible in all samples with characteristic peaks at 1350 and 1550 cm^{-1}.

Single crystals of X-ray quality were generated for **ONBTPS**, **BONBMPS**, **TONBES**, and **TONBPS** by using a mixture of chloroform and hexanes for crystal growth. Samples were mounted and studied for their X-ray crystal structures. They

https://doi.org/10.1021/acsomega.4c04837
ACS Omega 2024, 9, 40650−40664

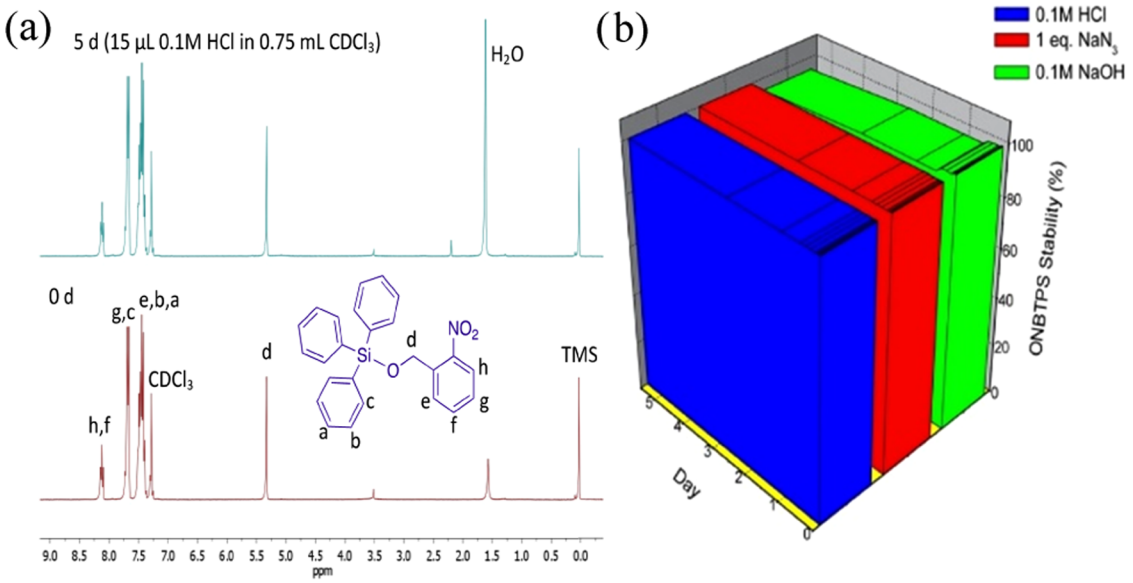

Figure 2. Stability of ONBTPS, (a) ^{1}H NMR before and after treatment with 0.1 M HCl for 5 days. (b) Treatment with 0.1 M HCl, 0.1 M NaOH, and 1 equiv of NaN_3.

were kept at 100.0° K during data collection and the structure was then solved and refined. The crystallization data for each of these samples are summarized in Table S4 and was used to generate the models of the crystal structures as shown in Figure 1. Crystal data for **TONBPS** was identified to have an orthorhombic structure where the final R_1 was 0.0366 ($I > 2\sigma(I)$), wR_2 was 0.0957, and Goodness of Fit (GooF) was 1.059 for all data, suggesting that the model and theoretical calculations aligned well. Crystal data for **DONBMPS**, **TONBES**, and **ONBTPS** were all identified to have monoclinic systems with final R_1 values of 0.0367, 0.0261, and 0.0394 ($I > 2\sigma(I)$), respectively, where wR_2 was 0.0961, 0.0689, and 0.1096 for all data in each set with GooF values of 1.036, 1.097, and 1.039 all suggesting that the models accurately represent the calculated structures. Ellipsoid models are included since anisotropic methods were used to solve the structures (Figures 1 and S44−S47). Only a small selection of samples was able to form single crystals, those that could order effectively through $\pi-\pi$ stacking. This was evident from the initial crystal unit modeling of **TONBES**, which showed four molecules layered with the 2-nitrosobenzyl alternating in a semiplanar style.

One of the objectives of this work was to safeguard the silicon core from untimely hydrolysis and condensation since alkoxysilane compounds (namely those containing methoxy or ethoxy groups) have a high propensity for self-polymerization in aqueous environments.[38] We anticipated that the **ONB** group would show better protection of the silicon core (versus ethoxy groups) against hydrolysis in acidic/basic conditions as well as nucleophilic attack via the use of sodium azide. To demonstrate this stability, we chose **ONBTES** and **ONBTPS** as model systems. The stability of **ONBTPS** in Figure 2, when dissolved in $CDCl_3$, was observed in the presence of 0.1 M HCl and 0.1 M NaOH for five and a half days. It also exhibited similar stability when mixed in a 1:1 molar ratio with sodium azide in dimethyl sulfoxide (DMSO) (5 days at room temperature and then 24 h at 40 °C). The ethyl derivative (**ONBTES**) has poorer stability than the phenyl derivative (**ONBTPS**) due to less steric crowding around the Si atom, especially against basic solutions. Despite **ONBTPS**'s high stability, it was found that reactions with fluoride ions in THF (Tetrabutylammonium fluoride, TBAF) still occur due to their small size and very high affinity for silicon; however, this can be used as an alternative **ONB** removal strategy if needed.

Photolysis for the deprotection of **ONBRSs** was initiated with exposure of the compounds to UV light (~250−400 nm, mercury arc lamp, UV/vis Figures S48−S61). This deprotection step specifically occurs in the **ONB** substituent, and subsequently leads to the cleavage of the O−C bond, resulting in the formation of a silanol anion ($Si-O^-$) and a nitrosoaldehyde compound (**NsBAld**),[14,23] which serves as the primary byproduct of photolysis. In the presence of water, hydrogen is abstracted by the silanol anion ($Si-O^-$) to obtain silanol (Si−O−H). To promote the subsequent condensation steps to link silanols, **DBTDL** was added, which is a widely used catalyst for silanol polymerization to form disiloxane, RTV-siloxane, and silsesquioxane structures with water as a byproduct.[39−41] Disiloxane, denoted as $R_3SiOSiR_3$, was the resultant compound formed from the photoreaction of **ONBTES** or **ONBTPS**. Siloxane, specifically in the form of $(-OSiR_2-)_n$, was the resultant photoproduct derived from **BONBDES**, **BONBDPS**, or **BONBMPS**. Silsesquioxanes, $(RSiO_{3/2})_n$, were formed as a result of the photoreaction of **TONBES** or **TONBPS**. To demonstrate the deprotection/coupling process, a solution of **ONBTES** in wet acetonitrile (Figure 62A) was subjected to irradiation for 6 h. The observed transformation of the colorless solution into a dark brown color signified the successful synthesis of **NsBALd**. Analysis of pre- and postphotolysis solutions by UV−vis absorption spectroscopy revealed characteristic absorption patterns for **ONBTES** (black) and **NsBALd** (red).[14] The deprotection process was also demonstrated for **ONBTES** using $CDCl_3$, with 1 equiv of H_2O, by following deprotection over 1 h (Figure S62B), which demonstrated that $CDCl_3$ could be used for NMR-based kinetic studies for deprotection processes. Note that NMR is used to follow deprotection due to difficult deconvolution of peaks in UV/vis, despite apparent faster deprotection in a quartz cuvette

https://doi.org/10.1021/acsomega.4c04837
ACS Omega 2024, 9, 40650−40664

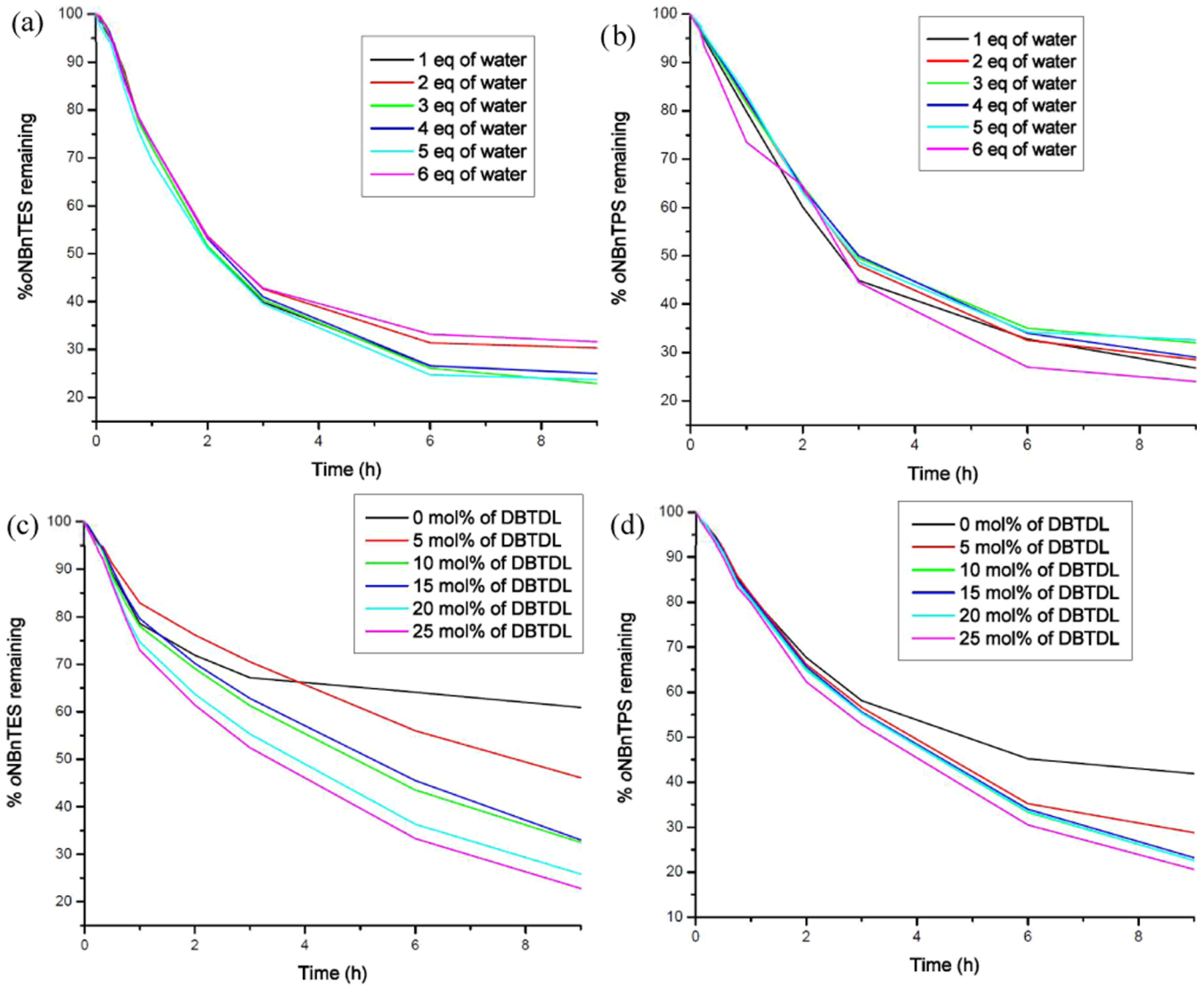

Figure 3. Plots depicting the hydrolysis of ONBRSs in varying equivalents of water and DBTDL for ONBTES and ONBTPS for several hours (0−9). (a) ONBTES hydrolysis evaluation in 1−6 equiv of water. (b) ONBTPS hydrolysis evaluation in 1−6 equiv of water. (c) ONBTES condensation evaluation in 0−25 mol % of DBTDL. (d) ONBTPS condensation evaluation in 0−25 mol % of DBTDL.

The photoreaction of **ONBRS** necessitates the presence of water to facilitate hydrolysis, whereas **DBTDL** is used to assist in the condensation/coupling stage. In the absence of any references providing adequate equivalents of water and **DBTDL** to aid polymer formation during **ONBRS** photolysis, ^{1}H NMR investigations were conducted to study the photolysis of single PPG model **ONBTES** and **ONBTPS** with a concentration of 0.55 M (in $CDCl_3$). The solutions were prepared and stored in glass NMR tubes. The NMR tubes were positioned inside a 3D-printed NMR tube holder, situated at a distance of 20 cm from the light source. We anticipated that the amount of water and the number of photocage groups in the **ONBRS** photodecomposition reactions should be at minimum equivalent to the number of alkoxy groups, enough to lead to the conversion of the silyl ether to silanol. We found that using less than 1 equiv does not provide enough water for complete conversion. Taking ^{1}H NMR measurements after 5, 10, 15, 30, and 45 min and 1, 2, 3, 6, and 9 h in each sample during the photolysis study, with 1−6 equiv of water, we found that effective conversion takes place with 1 equiv as shown in Figure 3. Note that the nontraditional PPG removal solvent of $CDCl_3$ was chosen due to allowing solubility of all **ONBRS** derivatives and that these are relative results since glass NMR tubes absorb a reasonable quantity of UV photons, meaning that reactions appear slower than without the glass barrier. This is in contrast to the conventional procedure of using a 4:1 acetonitrile to water ratio (V/V) commonly used for the removal of **ONB** groups, which happen within 30 min.[23] Water reduction was important to aid solubility and improve subsequent condensation reactions post deprotection.

Following the same hydrolysis evaluation procedure, a series of experiments were performed using varying concentrations (0, 5, 10, 15, 20, and 25 mol %) of the catalyst, **DBTDL**, to determine the optimal conditions needed for water-limited polymerization of **ONBTES** and **ONBTPS** (Figure 3). While the photolysis of **TONBPS** exhibited a decomposition rate 1.5 times higher (58.1%) compared to **TONBES** (39.1%) for 9 h in the absence of the catalyst, the inclusion of **DBTDL** had a discernible influence on the degradation of both compounds, as the ethyl derivative decomposed to 53.9% (1.3 times faster) and the phenyl derivative decomposed to 71.2% (1.2 times

https://doi.org/10.1021/acsomega.4c04837
ACS Omega 2024, 9, 40650−40664

faster) with the addition of 5 mol % of **DBTDL**. Even though the decomposition of these structures has a proportional relationship with the catalyst amount, especially with the ethyl derivative, the most beneficial ratio was determined to be 10 mol %, as shown by decomposition rates of 67.5 and 77.4% for **ONBTES** and **ONBTPS**, respectively. Therefore, we suspect that the binding of the tin catalyst to the silyl ether oxygen aids in the removal of the PPG by increasing the electron-withdrawing potential of the system.

Further experiments were performed to optimize the dimerization rate of mono PPG-functionalized **ONBRS**s (**ONBTES** and **ONBTPS**) in a different solvent (CD_3CN) with 1eq water and 10 mol % **DBTDL**. The deuterated version of acetonitrile (CD_3CN) was used to monitor the reaction by NMR. Photolysis was also investigated in CD_3CN for **BONBDES** and **ONBTES** (**ONBTPS** was insoluble). It was found that both rates were less efficient in comparison to those in the $CDCl_3$ studies. Additionally, the influence of water quantity on the polymerization rate of **ONBTES** in CD_3CN with 10 mol % of catalyst for 9 h was examined due to the miscibility difference between CD_3CN (complete) and $CDCl_3$ in water. The results after 3 trials (1, 3, 6 equiv of water) exhibited that exceeding 1 equiv of water yielded comparable cleavage percentages, implying that the duration of exposure had a more significant influence than the water quantity.

We analyzed the overall optimal conditions for the photolysis of the **ONBRS**s through a series of 28 trials. Among these trials, 24 used $CDCl_3$ as shown in Table S5, and the remaining 4 employed CD_3CN as documented in Table S6. The results of these experiments revealed that the use of $CDCl_3$ with 1 equiv of water and 10 mol % of **DBTDL** yielded higher photodecomposition. Therefore, a study was undertaken to examine the photodecomposition of **ONBRS**s and calculate the photophysical properties at a concentration of 0.55 M, under optimal conditions (Table 1). Pursuing the same approach as that used for previous analyses, the effects of photolysis on **ONBRS**s were monitored by UV/vis and NMR. Table 1 presents the obtained outcomes, including the wavelength maxima (λ_{max}), the initial rate constant of the photodecomposition (k_{int}), the molar absorption coefficient (ε), and relative quantum yields (Φ, lowered due to glass tube effects).

Table 1. Photophysical/Chemical Properties of ONBRSs in $CDCl_3$ with 1 equiv of Water and 10 mol % of DBTDL

compound	λ_{max} (nm)	$\varepsilon \times 10^4$ (M^{-1} cm^{-1})	k_{int} value $\times 10^{-3}$ (s^{-1})	Φ (% ± STDEV)
ONBTES	266	0.50	3.26	4.5 ± 1.7
ONBTPS	265	0.02	2.89	3.0 ± 2.2
BONBDES	262	1.12	10.39	3.5 ± 1.7
BONBDPS	265	0.19	1.44	2.9 ± 2.2
BONBMPS	266	0.14	3.71	3.2 ± 2.0
TONBES	265	0.24	8.01	2.5 ± 2.2
TONBPS	264	0.24	1.18	2.7 ± 2.1

Equation 1 was used to analyze the kinetic behavior of the photodecomposition reactions; where $[P]$ is the change in the concentration of the product, t denotes the irradiation time, $[R]$ is the initial concentration/reactant concentration, and k is the rate constant of the photodecomposition.[42]

$$\frac{-\mathrm{d}[R]}{\mathrm{d}t} = \frac{\mathrm{d}[P]}{\mathrm{d}t} = k[R] \quad (1)$$

A comparative kinetic study was performed on all derivatives; see Table 2 and Figures 4 and 5. Triethyl and triphenyl derivatives, namely, **ONBTES** and **ONBTPS**, were explored in most detail. Initial change within the first 15 min for each sample was more linear than further time points, which is expected due to byproduct absorption effects. The initial k values, represented as k_{int}, (0 to 15 min) for triethyl and triphenyl were 3.30×10^{-3} s^{-1} and 2.90×10^{-3} s^{-1}

Table 2. Kinetic Rate Comparison for ONBRS Photodecomposition in $CDCl_3$

	k ($\times 10^{-3}$ s^{-1})			
ONBRS	0–15 min	0.25–1 h	1–2 h	average
ONBTES	3.30	13.1	6.80	7.7
ONBTPS	2.90	5.30	3.50	3.9
BONBDES	10.4	10.6	5.40	8.8
BONBDPS	1.40	4.40	3.20	3.0
BONBMPS	3.70	6.70	5.20	5.2
TONBES	8.00	4.40	3.00	5.1
TONBPS	1.20	3.60	3.90	2.9

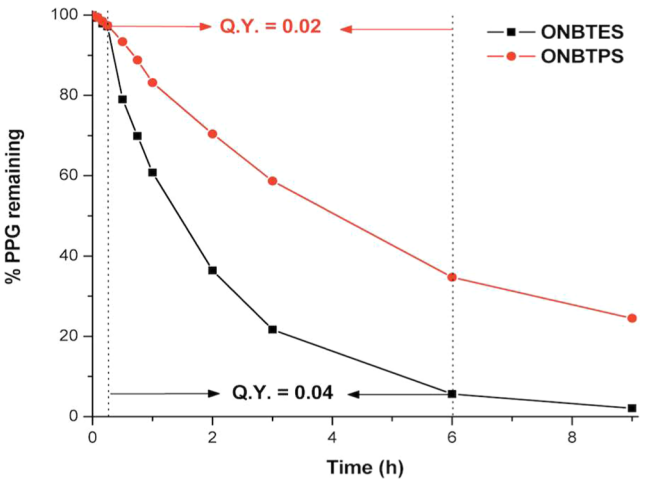

Figure 4. Photodecomposition of ONBTES and ONBTPS in $CDCl_3$.

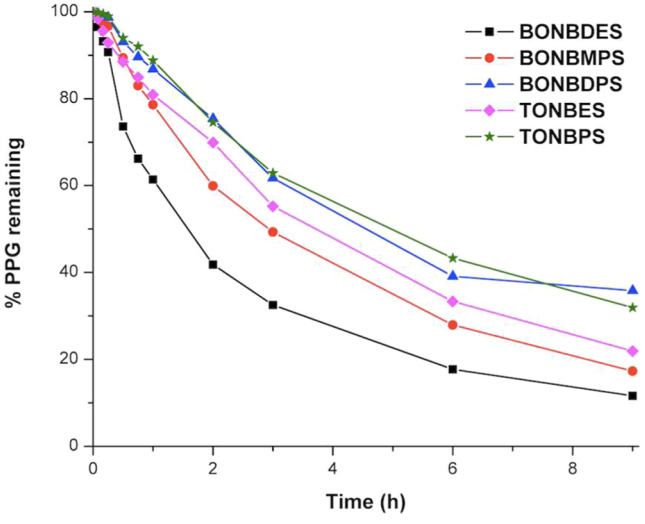

Figure 5. Photodecomposition of di- and trifunctionalized **ONBRS**s in $CDCl_3$.

https://doi.org/10.1021/acsomega.4c04837
ACS Omega 2024, 9, 40650−40664

respectively. However, we observed a significant change in the next transition point from 15 min to 1 h where the k value for triethyl was found to be 13.10×10^{-3} s^{-1} while for triphenyl it was 5.30×10^{-3} s^{-1}. The rate of decomposition was 2.5 times greater in the triethyl derivative during this major transition in product formation. In the time interval between 1 to 2 h, the k value was linear for both derivatives (triethyl 6.80×10^{-3} s^{-1} and triphenyl 3.50×10^{-3} s^{-1}). We believe this is due to competing absorbance between a large number of phenyl rings, limiting the efficiency of the photoreaction. To summarize the monofunctionalized silanes' kinetics, **ONBTES** yielded better photoproduct conversion compared to **ONBTPS** at 9 h (98 versus 76%). Both showed nonlinear behavior, especially after the first 15−20 min which we attribute to the formation of the nitroso-aldehyde byproduct (**NsBAld**) which causes the solution to turn dark brown in color, hence slowing the rate of PPG removal.

Difunctionalized silanes k_{int} values of 10.4×10^{-3} s^{-1}, 3.7×10^{-3} s^{-1}, and 1.4×10^{-3} s^{-1} were found for **BONBDES**, **BONBMPS**, and **BONBDPS**, respectively, indicating that the reactivity of these silanes toward the photodecomposition process decreases with increasing phenyl attached to Si. During the time interval ranging from 15 to 60 min, the **BONBDES** maintained a rapid photodecomposition rate of 10.6×10^{-3} s^{-1}. However, both the **BONBMPS** and **BONBDPS** showed lower rates with increasing phenyl, with **BONBMPS** reaching 6.7×10^{-3} s^{-1} and **BONBDPS** reaching 4.4×10^{-3} s^{-1}. The k values for all three (5.4×10^{-3} s^{-1} for **BONBDES**, 5.2×10^{-3} s^{-1} for **BONBMPS**, and 3.2×10^{-3} s^{-1} for **BONBDPS**) fell after irradiating them for 60 to 120 min, indicating a decrease in the response rate with time. Overall, **BONBDES** had the highest initial response rate, but **BONBMPS** demonstrated the most pronounced rise in the reaction rate as time progressed. **BONBDPS** exhibited a consistent response rate across the investigated time intervals.

The k values of **TONBES** at 8.00×10^{-3} s^{-1} (0−15 min), 4.40×10^{-3} s^{-1} (15−60 min), and 3.00×10^{-3} s^{-1} (1−2 h) demonstrated a declining rate trend over 120 min. In contrast, **TONBPS** at 1.20×10^{-3} s^{-1} (0−15 min), 3.60×10^{-3} s^{-1} (15−60 min), and 3.90×10^{-3} s^{-1} (1−2 h) exhibited an increase in response rate throughout the same period. Nonetheless, the total rate of product formation for **TONBES** remained higher than that of **TONBPS** toward the end of the irradiation time.

To summarize the overall kinetics, the **ONBRS**s k_{int} values were lower (showed induction) compared to the rates over 15−120 min; after 2 h the rates slowed due to byproduct formation which cuts off irradiation due to its dark color. We observed that the phenyl group attached to the silane compound acted as a stabilizing factor against photodecomposition and slowed PPG removal.

The quantum yields (Φs) were obtained by exposing NMR tubes, containing each **ONBRS**, to irradiation at various time intervals, while simultaneously observing the outcomes using ^{1}H NMR spectroscopy, see the SI. Note that these values are smaller than typical for **ONB** removal (∼45%)[14] due to $CDCl_3$ as a solvent and lower UV region photon flux than expected due to glass NMR tubes, ∼15−20 mW/cm^2 reaching the sample, but richer in visible than UV, due to glass blocking. The equation below was used to obtain relative Φs of photorelease for all monomers in this study (eq 2). Avoiding induction, the averages of Φ values for all of the compounds are shown in Table 1 and were found over a range from 30 min to 6 h. Due to both solvent and glass transmission effects, the values are all below 5% and have high standard deviations (Table 1). The indication of ethyl derivatives (**ONBTES, BONBDES, TONBES**) having higher Φs than phenyl derivatives (**ONBTPS, BONBDPS, TONBPS**) was attributed to the phenyl ring absorbing part of the light. For example, the Φ of **ONBTES** was higher (∼4.5%) than the Φ of **ONBTPS** (∼2.5%) as shown in Figure 4. The attached methyl and phenyl groups in the hybrid **ONBRS**, **BONBMPS**, represent the middle range of Φ values for difunctionalized **ONBRS**s. We also observed an inverse relationship between Φ and the number of **ONB**s on each derivative, which represents Φs fall when increasing the number of **ONB**s on each molecule, i.e., increased electron density lowers efficiency. Overall, the Φs indicated that the photolysis of ethyl derivatives was more efficient than phenyl derivatives, but that Φs tended to equalize with increasing PPG on silicon.

$$\Phi = \frac{d[P]/dt}{I} \tag{2}$$

The photodeprotection process of the monomers (**ONBRS**s) shown in Scheme 2 was conducted in $CDCl_3$ and CD_3CN (where able), following the aforementioned experimental conditions used to derive kinetic and Φ values. A focus was not given to isolating each of the many products generated *in situ*; however, for completeness, we supply the characterization data of the mixed products in the ESI for GPC, TGA, and FTIR (Figures S63−S86 and Table S8). This includes derivatives of $[R_3SiOSiR_3$, $(-OSiR_2-)_n$, and $(RSiO_{3/2})_n]$. Most notably, the FTIR spectra of photoproducts provided evidence for the formation of Si−O−Si bonds with peaks within the range of 1000−1050 cm^{-1}. These spectra also revealed the presence of aldehyde peaks corresponding to the byproduct (**NsBAld**), with the C═O bond peak seen within the range 1680−1720 cm^{-1} and the aldehyde C−H bond peak within the range 2700−2800 cm^{-1}. GPC analysis also shows the formation of oligomeric species, which are more finely tuned in the next section.

We will use three examples to demonstrate the polymerization (unoptimized) ability of these systems, with further examples being the subject of a follow-on manuscript. Our first example of a use-case for these materials is the polymerization of **BONBDPS** toward siloxane polymers. Though many such reactions were conducted for kinetic studies, we did not follow each to polymer formation. The diphenyl-containing derivative was chosen due to its ability to be visualized well in the GPC because of its strong absorption. We used wet acetonitrile in a quartz cuvette and 24 h of irradiation time for these studies to verify the reaction completion and efficiency. The extended duration of the reaction and added **DBTDL** (added after 8 h) aided the condensation reactions, resulting in a poly(diphenylsiloxane) as shown in the GPC of Figure 6. A comparison of starting materials (black) versus intermediates (red), and final products (blue) is shown. The polymer peak at 31 min represents polymer structures having Mn = 3300 Da, Mw = 4500 Da, and a PDI = 1.4. Note that it is anticipated that diphenyl cyclic siloxanes would form during this process and are likely present at 33−35 min. Since all characterization of the starting **BONBDPS** points to high purity, we suspect the double peaks come from the degradation of the monomers either by room light or from the lamp in the UV/vis detector of the GPC system which irradiates the samples at 265 nm. The inset of this image shows the change in color from

https://doi.org/10.1021/acsomega.4c04837
ACS Omega 2024, 9, 40650−40664

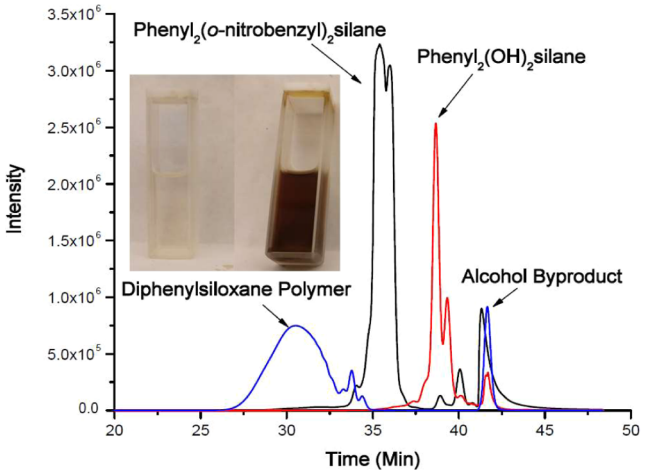

Figure 6. GPC of BONBDPS before (black), after photoreaction (red), and blue after 24 h polymerization w/DBTDL (Mn = 3300 Da, Mw = 4500 Da, PDI = 1.4). Inset—reaction mixture before (left panel) and after (right panel) photoreaction. Peak shoulders to the right are believed to be from UV/vis detector-induced degradation (265 nm).

transparent to dark brown, indicative of the removal of the **ONB** group. The (partial) hydroxylated intermediate (red) was taken after 8 h of irradiation, suggesting that full deprotection takes place before polymerization occurs. This experiment was conducted at room temperature with 10 mol % **DBDTL** added from the beginning of the photoreaction.

The second example combines both **BONBDPS** and **TONBPS** in a 1:1 ratio to make a slightly cross-linked network and assess the performance of mixed systems. This sample was irradiated for 9 h in $CDCl_3$ with 5 equiv of water relative to reactive groups (Table S6). By TGA, we observed that the initial decomposition $T_{d5\%}$ was 165.22 °C, suggesting incomplete reactivity to form a fully condensed polymer, and then a final CY of 13.9% was obtained (Figure S87). Although it is difficult to predict the theoretical CY for these systems, we still expected a value above 20%. The FTIR spectra (Figure S88) show a broadening of the peak at ∼1100 cm^{-1} suggesting Si−O−Si bonds beyond alkoxysilanes, the peaks at ∼1700 cm^{-1} suggest carbonyl formation from the photobyproduct, and 1510 cm^{-1} NO_2 diminishing suggest photoreaction of the protecting group. This material resulted in a mostly insoluble gel product that could not be characterized by GPC.

The third example uses **TONBES** to form poly(ethylsilsesquioxane) $(EtSiO_{3/2})_n$ gels through photolysis and polymerization. This experiment was conducted using THF as the solvent to aid in solubilizing the sol−gel process during network structure building (0.55 M **TONBES** in a covered crystallizing dish, 3 equiv water, 10 mol % **DBTDL**, and 24 h irradiation). The product was an insoluble brown sludge, which was rinsed with hexanes and acetone to remove byproduct residues (Figure 7). It was then vacuum-dried overnight at room temperature. The TGA spectrum, as shown in Figure S89, exhibited a ceramic yield of 69.6% (74.0% theory) and $T_{d5\%}$ at 321.6 °C, verifying successful conversion. FTIR analysis, as shown in Figure S90, revealed the presence of Si−O−Si and C−H bonds. Both tools confirm effective silsesquioxane structure formation. 3D confocal microscopy was also used to visualize the product of this reaction. The microscopy images of **TONBES** are presented in Figure S91a−c at magnifications of X40, X500, and X1000. Figure S91e depicts the $(EtSiO_{3/2})_n$ particle with the red box showing the region for 30-fold magnification (Figure S91d). The elemental analyzer detected varying percentages of silicon (Si), carbon (C), hydrogen (H), oxygen (O), and tin (Sn, from **DBTDL**) at seven different locations, as illustrated in Figure S91f and Table S9. This analysis revealed the presence of $(EtSiO_{3/2})_n$ (the desired product), **NsBAld** (the byproduct), and **DBTDL** (catalyst) in the sample. Figure S91g represents the two-dimensional (2D) version of Figure S91e.

The **ONBRS** such as **TONBPS** and **TONBES** have applications in surface functionalization and coatings. As a demonstration, we chose to modify three different surfaces, including a silica thin layer chromatography plate (TLC) with fluorescent backing, a glass microscope slide, and an undoped silicon wafer. The surfaces of these objects were modified as outlined below with photolysis and coupling of either **TONBPS** or **TONBES** in wet THF and a **DBTDL** catalyst. This method overcomes many of the acid/base methods typically used for surface modification and allows for neutral patterning of multiple surfaces.[43−45] In general, surfaces containing hydroxyl groups either need to be naturally present or must be induced by chemical methods. Hydroxyls are then coupled with an **ONBRS** modifier with irradiation, giving

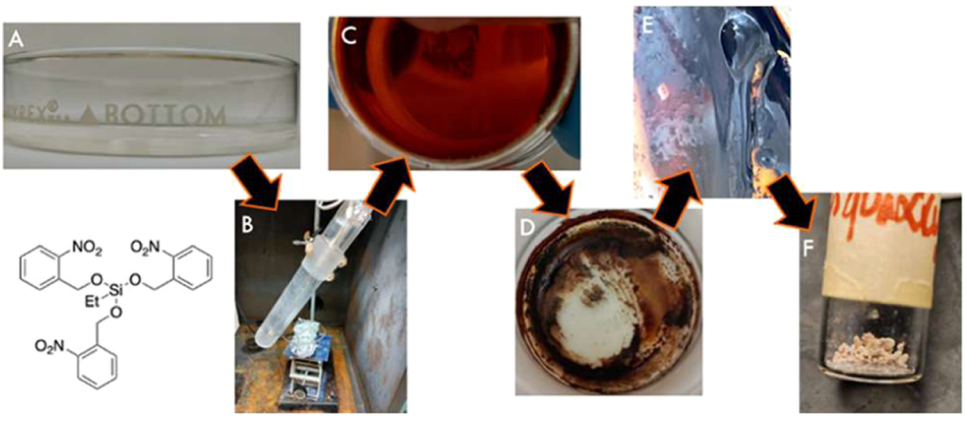

Figure 7. Setup for the polymerization of **TONBES** to polyethylsilsesquioxane by photolysis in THF, (A) 0.55 M TONBES in THF, H_2O, and DBTDL; (B) photolysis setup; (C) solution after photolysis; (D) after evaporation; (E) close up after solvent evaporation; and (F) after rinsing with hexanes and acetone.

https://doi.org/10.1021/acsomega.4c04837
ACS Omega 2024, 9, 40650−40664

covalently attached functionality only where irradiated, for potential applications in photopatterning/lithography.[46−48] In this study, hydrophilic hydroxylated surfaces are converted to more hydrophobic surfaces.

TONBPS was used to modify a TLC plate as its fluorescent backing makes it easy to observe where aromatic functionalization has occurred since masked regions will maintain fluorescence (Figure 8). We used wooden BGSU letters as a

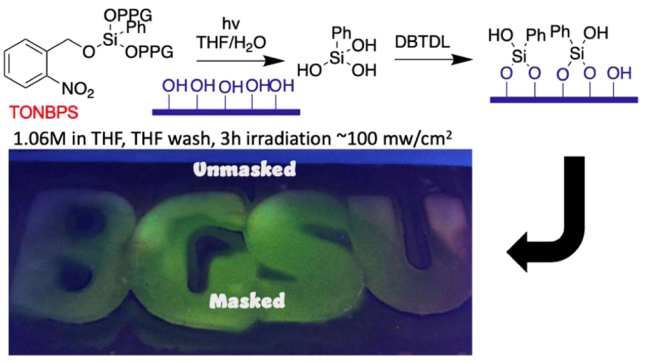

Figure 8. Surface functionalization of silica gel on a glass plate by using **TONBPS**.

mask (2 cm height) to create the mask and UV irradiated a 1.06 M solution of **TONBPS** with 3 equiv of H_2O and 10 mol % of **DBTDL** in THF for 3 h, followed by THF washes. Figure 8 shows the results of this study, with clear distinctions between masked and unmasked regions, indicating that photolysis and coupling processes have occurred.

A glass slide and a silicon wafer were also used to further demonstrate surface functionalization using this technique. The surfaces of these substrates are more naturally intermediate to low polarity. The surface of these substrates was cleaned with acetone/ethanol sonication for 10 min and was made more polar by increasing the level of OH surface groups using an acid solution containing H_2SO_4 and H_2O in a 7:3 ratio, submerged for 2 h each, and then rinsed with fresh water. The samples were then partially covered with foil to protect some of the surface from functionalization; therefore, a direct test of hydrophobicity could be compared. The samples were submerged in 1.06 M **TONBES**, 3 equiv of H_2O, and 10 mol % of **DBTDL** in 1.5 mL of THF, followed by UV irradiation at room temperature for 3 h (Scheme S1). Once completed the samples were rinsed thoroughly with THF and hydrophobicity was tested by sessile drop static contact angle measurement.[49] A drop of water was placed on both sides (unexposed and exposed) of the samples' surface. A static contact angle (SCA) of each sample (Table 3) was measured (Figure 9). The SCA of the unexposed glass surface (OH functionalized) was 76.4°, making it hydrophilic, whereas the SCA of the exposed side was 97.0°, indicating that the surface

Table 3. Contact Angle of the Glass Plate and Silicon Coupon before and after Surface Modification Using TONBES

material sample	static contact angle − (SCA)
untreated glass	76.4° (±0.5)
exposed glass	97.0° (±0.3)
untreated silicon wafer	57° (±1.6)
exposed silicon wafer	90.4° (±0.1)

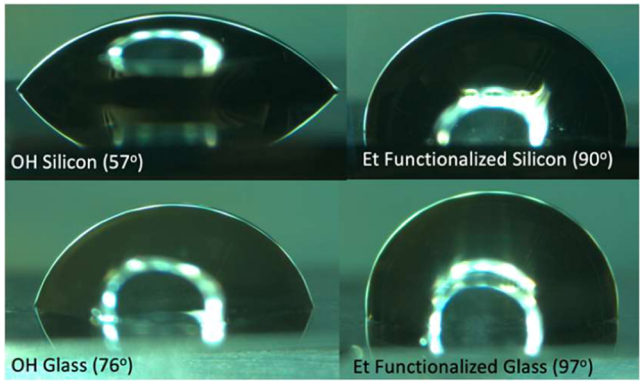

Figure 9. Microscopy image of both sides of the etched glass plate after modification. (a) unexposed side and (b) exposed side.

was modified to make it hydrophobic. For the silicon coupon, the SCA was 57.0 and 90.4° for the unexposed and exposed sides, respectively, suggesting that a slight hydrophobic surface was obtained. These studies further demonstrate the scope of uses **ONBRS**s have.

CONCLUSIONS

In this study, we demonstrated a productive procedure (>80% yield) for protecting ethyl (aliphatic), phenyl (aromatic), and methyl-phenyl silanes using the 2-nitrobenzyloxy (**ONB**) group at 0 °C in the presence of triethylamine (TEA) to form R-alkoxysilanes (**ONBRS**s) with photoreleasable alkoxy groups, giving spatial and temporal control to alkoxysilane chemistry. We also showed that they were highly stable in mild acid, in the presence of a nucleophile (azide), and moderately stable in basic solutions.

Photolysis conditions were investigated for water and catalyst needed to effect transformation for **ONBTES** and **ONBTPS** and optimally were found to deprotect to >90 and 70%, respectively, within 9 h in $CDCl_3$ using a medium-pressure mercury lamp in the presence of 1 equiv of water and 10 mol % of **DBTDL**. This study showed that $CDCl_3$ is an adequate solvent for these systems even with limited water compared to conventional deprotection of **ONB** groups in 4:1 CH_3CN/H_2O. Overall, our photochemical investigation into quantum efficiencies (Φ) is a bit ambiguous, but there appears to be a trend toward those with ethyl R-groups being more responsive than phenyl-containing moieties, which we attribute to competitive absorption of the phenyl rings. Additionally, we have demonstrated a series of material applications for these processes, exposure to $CDCl_3$ for 9 h was not sufficient, so **ONBRS**s were irradiated. We have shown the effective formation of oligomeric diphenylsiloxanes using CH_3CN and 24 h irradiation (Mw = 4500 Da and PDI = 1.4). Mixed functional cross-linked polymers were demonstrated by combining **BONBDPS** (difunctionalized) and **TONBPS** (trifunctionalized). This led to insoluble siloxane gel materials, demonstrating an effective reactivity. To make silsesquioxane materials, **TONBES** was irradiated for 24 h in THF (chosen for solubility of intermediates) to generate polyethylsilsesquioxane, confirmed by FTIR and TGA. Lastly, **ONBRS**s use was demonstrated for surface patterning and functionalization applications through the selective functionalization of silica (TLC), glass, and silicon metal surfaces. The method was effective for surface modifications and opened new doors for

https://doi.org/10.1021/acsomega.4c04837
ACS Omega 2024, 9, 40650−40664

the spatial and temporal control of alkoxysilane reactions on surfaces and other advanced applications.

Future work will continue on the development of other PPG R-alkoxysilanes with diverse functionalities and PPG-functionalized siloxane/silsesquioxane polymer systems.

MATERIALS AND METHODS

General Information. All chemicals were purchased from commercially available sources and used without any further purification unless otherwise stated in the experimental details below. 2-nitrobenzyloxy silane derivatives [$(2\text{-nitrobenzyloxy})_{n=1-3}(R)_{m=1-3}$silanes, **ONBRSs**] were synthesized in the dark and/or a UV-blocked environment to prevent premature deprotection of the silanes and the siloxanes. A mixture of benzophenone, sodium metal (Na), and tetrahydrofuran (THF) was refluxed for 4 h and then distilled to obtain dry THF. Characterization for all synthesized compounds is given throughout the manuscript and in the Supporting Information.

Analytical Methods. *Fourier Transform Infrared Spectroscopy (FTIR).* Spectra were obtained on a Thermo Scientific Nicolet iS5 Fourier transform infrared spectrometer. Attenuated total reflection (ATR) was used. Without further sample preparation, solid samples were placed on a ZnSe crystal and scanned from 4000 to 550 cm^{-1} for 16 scans with 0.121 cm^{-1} data spacing.

Thermal Gravimetric Analysis (TGA). Thermal stabilities and ceramic yields (CYs) of samples in air were measured on a TA Instruments TGA-50. Samples of 4−10 mg were placed into an alumina pan and heated from 25 to 1000 °C at a rate of 10 °C/min with 200 mL/min air-flow.

Gel Permeation Chromatography (GPC). GPC analyses were performed on a Shimadzu LC-10 system (LC Solutions Software) equipped with a set of Waters Styragel columns (HR 0.5, 1, 3, and 4) with a Shimadzu RID-10 RI detector and SPD-10a UV detector with THF as an eluent at a 1 mL/min flow rate. This system was calibrated using a set of eight polystyrene standards, with toluene used as an internal reference.

Nuclear Magnetic Resonance (NMR). ^{1}H NMR and ^{13}C NMR spectra were obtained using a 500 MHz Bruker Avance spectrometer. Chemical shifts are reported relative to residual solvent signals ($CDCl_3$, ^{1}H: δ 7.26; ^{13}C: δ 77.36; CD_3CN, ^{1}H: δ1.96; ^{13}C: δ 1.79, 118.26). ^{1}H NMR data are assumed to be first order and the multiplicity is reported as "s" = singlet and "m" = multiplet, etc. $^{29}Si\{^{1}H\}$ and ^{1}H NMR spectra were recorded on a Bruker Avance 300 spectrometer (^{29}Si: 59.6 MHz) using glass peak at −110[1,2] ppm or tetramethylsilane as external or internal references. ^{1}H NMR data was used to calculate the physical properties of the photoproducts.

UV−Vis Spectrometry. UV/vis measurements were recorded on a Shimadzu UV-2600 spectrometer with a resolution of 1.0 nm with 1 s integration time. All of the measurements were performed using a quartz cuvette with a path length of 0.5 cm at room temperature. Concentrations were on the order of (10^{-6}−10^{-7} M). Molar extinction coefficients (ε, M^{-1} cm^{-1}) were determined by plotting a standard curve with concentrations ranging from 10^{-5}−10^{-6} M.

Single Crystal X-ray Diffraction (SC-XRD). Single crystals of $C_{27}H_{23}N_3O_9Si$ tris(2-nitrobenzyloxy)phenylsilane, $C_{21}H_{20}N_2O_6Si$ bis(2-nitrobenzyloxy)methylphenylsilane, $C_{23}H_{23}N_3O_9Si$ ethyltris(-2-nitrobenzyloxy)silane, and $C_{25}H_{21}NO_3Si$ 2-nitrobenzyloxytriphenylsilane were formed using chloroform and hexane. A suitable crystal was selected and mounted on a micromesh and then analyzed with a Bruker D8 Quest equipped with an APEX-II CCD diffractometer. The crystal was kept at 100.0 K during data collection. Using Olex2,[3] the structure was solved with the XT[4] structure solution program using Intrinsic Phasing and refined with the SHELXL[5] refinement package using Least Squares minimization. Images and models were generated using Mercury (v2022.1.0).

Gas Chromatography-Mass Spectrometry (GC−MS). GC−MS measurements were carried out on a Shimadzu GC-2010 gas chromatograph (30 m ZB-5 ms column, 60−350 °C) linked with a Shimadzu GCMA-QP 2010 Plus mass spectrometer. One mg of sample was dissolved in 1 mL of chloroform and then 10 mL of this solution were further diluted in an additional 1 mL of solvent before injection.

High-Resolution Mass Spectrometry (HRMS). HRMS was conducted at North Dakota State University on a SYNAPT G2-Si by Waters instrument in Positive Resolution mode, scanning range 100−1200 Da. All samples were dissolved in 1 mL of THF. 50 mL of each THF solution were transferred into a new vial. 1.6 mL MeOH (mass spec grade) were added to each vial before injection into the ESI.

Laser-Based Elemental Analysis. The percentages of each element in the ethylsilsesquioxane $(EtSiO_{3/2})_n$ sample were determined by the use of a Keyence VHX-7000 series digital microscope and a Keyence EA-300 laser-based elemental analyzer (both manufactured by Keyence Corporation of America and located in Broadview Heights, Ohio). Laser-induced breakdown spectroscopy was performed in air using a class I, 355 nm laser with a spot size of 10 mm.

Synthesis of $(2\text{-Nitrobenzyloxy})_{n=1-3}(ethyl/phenyl)_{m=1-3}$silanes (ONBRs). *General Procedure.* To a solution of $(chloro)_{n=1-3}(ethyl/phenyl)_{m=1-3}$silane (1 equiv) was dissolved in dry THF and added dropwise to a mixture of 2-nitrobenzyl alcohol ($n_{=1-3}$ × 1.2 equiv) with triethylamine ($n_{=1-3}$ × 1.2 equiv) in 40 mL of dry THF under nitrogen at 0 °C in the dark (wrapped in foil), followed by continuous stirring for 3 h. The solution was filtered to remove the undissolved. The solvent was removed under a high vacuum. The products of each reaction were purified as given below. All products were stored in foil-wrapped containers in the freezer before further study.

*2-Nitrobenzyloxytriethylsilane (**ONBTES**) from NaH.* To a solution of chlorotriethylsilane (628 mL, 3.7 mmol, 1 equiv) was dissolved in dry THF and added dropwise to a mixture of 2-nitrobenzyl alcohol (687 mg, 4.4 mmol, 1.2 equiv) with sodium hydride (0.11 g, 4.4 mmol, 1.2 equiv) in 40 mL of dry THF under nitrogen at 0 °C in the dark (wrapped in foil), followed by continuous stirring for 3 h. The solution was filtered to remove the undissolved. The solvent was removed under a high vacuum. The product was purified with silica gel chromatography (hexane/dichloromethane, 1:1) resulting in a yellow/golden oil at 74% yield (1.01 mL). ^{1}H NMR (500 MHz, $CDCl_3$) δ: 8.08−8.11 (d, 1H), 7.96−7.99 (d, 1H), 7.67−7.70 (t, 1H), 7.40−7.44 (t, 1H), 5.13 (s, 1H), 1.00−1.04 (t, 9H), 0.70−0.73 (q, 6H).

*2-Nitrobenzyloxytriethylsilane (**ONBTES**).* Chlorotriethylsilane (628 mL, 3.7 mmol, 1 equiv), 2-nitrobenzyl alcohol (687 mg, 4.4 mmol, 1.2 equiv), and triethylamine (626 mL, 4.4 mmol, 1.2 equiv) were mixed as given in the general procedure. The product was purified with silica gel chromatography (hexane/dichloromethane, 1:1) resulting in

https://doi.org/10.1021/acsomega.4c04837
ACS Omega 2024, 9, 40650−40664

a yellow/golden oil in 90.4% yield (1.01 mL). ^{1}H NMR (500 MHz, $CDCl_3$) δ 8.09−8.11 (d, 1H), 7.96−7.98 (d, 1H), 7.67−7.70 (t, 1H), 7.40−7.44 (t, 1H), 5.13 (s, 1H), 1.00−1.04 (t, 9H), 0.70−0.74 (q, 6H); ^{13}C NMR (125 MHz, $CDCl_3$) δ 146.46, 138.33, 133.78, 127.94, 127.37, 124.48, 61.76, 6.74, 4.41; ^{29}Si NMR (59.6 MHz, $CDCl_3$) δ 22.08; HRMS (ESI/QTOF) m/z $[M + H]^+$ calculated for $C_{13}H_{21}NO_3Si$ 267.1291, found 267.1298.

*2-Nitrobenzyloxytriphenylsilane (**ONBTPS**).* Chlorotriphenylsilane (717 mg, 2.4 mmol, 1 equiv), 2-nitrobenzyl alcohol (446 mg, 2.9 mmol, 1.2 equiv), and triethylamine (406 mL, 2.9 mmol, 1.2 equiv) were mixed as given in the general procedure. The product was purified with silica gel chromatography (hexane/dichloromethane 1:1) resulting in white crystals in 95.6% yield (0.95 g). ^{1}H NMR (500 MHz, $CDCl_3$) δ 8.11−8.15 (m, 2H), 7.68−7.73 (m, 7H), 7.46−7.51 (m, 3H), 7.42−7.45 (m, 7H), 5.34 (s, 1H); ^{13}C NMR (125 MHz, $CDCl_3$) δ 146.45, 137.54, 135.39, 133.94, 133.42, 130.36, 128.13, 128.08, 127.57, 124.62, 62.81; ^{29}Si NMR (59.6 MHz, $CDCl_3$) δ −10.53; HRMS (ESI/QTOF) m/z $[M + H]^+$ calculated for $C_{25}H_{21}NO_3Si$ 411.1291, found 411.1292.

*Bis(2-nitrobenzyloxy)diethylsilane (**BONBDES**).* The compound was obtained from mixing dichlorodiethylsilane (379 mL, 2.56 mmol, 1 equiv), 2-nitrobenzyl alcohol (471 mg, 3.07 mmol, 2.2 equiv), and triethylamine (428 mL, 3.07 mmol, 2.2 equiv) according to the general procedure. The product was purified with silica gel chromatography (hexane/dichloromethane 1:1) resulting in a white powder at 86.2% yield (0.862 g). ^{1}H NMR (500 MHz, $CDCl_3$) δ 8.03−8.05 (d, 2H), 7.89−7.91 (d, 2H), 7.63−7.67 (t, 2H), 7.38−7.41 (t, 2H), 5.20 (s, 4H), 1.08−1.11 (t, 6H), 0.82−0.87 (q, 4H); ^{13}C NMR (125 MHz, $CDCl_3$) δ 146.37, 137.36, 133.88, 127.74, 127.65, 124.55, 61.63, 6.47, 3.84; ^{29}Si NMR (59.6 MHz, $CDCl_3$) δ −1.99; HRMS (ESI/QTOF) m/z $[M + H]^+$ calculated for $C_{18}H_{22}N_2O_6Si$ 390.1247, found 390.1254.

*Bis(2-nitrobenzyloxy)diphenylsilane (**BONBDPS**).* The compound was obtained from mixing dichlorodiethylsilane (432 mL, 2.05 mmol, 1 equiv), 2-nitrobenzyl alcohol (378 mg, 2.46 mmol, 2.2 equiv), and triethylamine (344 mL, 2.46 mmol, 2.2 equiv) according to the general procedure. The product was purified by recrystallization using a combination of dichloromethane (DCM) and methanol (MeOH), which yielded the product as a white solid in 80.5% yield (805 mg). ^{1}H NMR (500 MHz, $CDCl_3$) δ 8.07−8.08 (d, 2H), 8.02−8.04 (d, 2H), 7.78−7.79 (t, 2H), 7.76−7.77 (d, 2H), 7.67−7.71 (t, 2H), 7.52−7.54 (t, 1H), 7.51 (s, 1H), 7.46−7.47 (t, 1H), 7.42−7.46 (m, 5H), 5.31 (s, 4H); ^{13}C NMR (125 MHz, $CDCl_3$) δ 146.51, 136.84, 134.83, 133.92, 131.24, 130.98, 128.26, 127.94, 127.79, 124.65, 62.25; ^{29}Si NMR (59.6 MHz, $CDCl_3$) δ −29.03; HRMS (ESI/QTOF) m/z $[M + H]^+$ calculated for $C_{26}H_{22}N_2O_6Si$ 486.1247, found 486.1253.

*Bis(2-nitrobenzyloxy)methylphenylsilane (**BONBMPS**).* The compound was obtained from mixing dichlorodiethylsilane (385 mL, 2.35 mmol, 1 equiv), 2-nitrobenzyl alcohol (794 mg, 5.18 mmol, 2.2 equiv), and triethylamine (723 mL, 5.18 mmol, 2.2 equiv) according to the general procedure. The product was purified by recrystallization using a combination of DCM and MeOH, which gives the product as a white powder in 93.6% yield (936 mg). ^{1}H NMR (500 MHz, $CDCl_3$) δ 8.07−8.09 (d, 2H), 7.95−7.97 (d, 2H), 7.739−7.74 (t, 1H), 7.726−7.729 (d, 1H), 7.42−7.53 (m, 5H), 5.26−5.27 (d, 4H), 0.59 (s, 3H); ^{13}C NMR (125 MHz, $CDCl_3$) δ 146.52, 136.97, 133.93, 132.97, 130.76, 128.26, 127.96, 127.76, 124.64, 61.97, −4.45; ^{29}Si NMR (59.6 MHz, $CDCl_3$) δ −14.06; HRMS (ESI/QTOF) m/z $[M + H]^+$ calculated for $C_{21}H_{20}N_2O_6Si$ 424.4840, found 424.1095.

*Tris(2-nitrobenzyloxy)ethylsilane (**TONBES**).* To a solution of trichloroethylsilane (257 mL, 1.94 mmol, 1 equiv) dissolved in dry THF was added dropwise to a mixture of 2-nitrobenzyl alcohol (955 mg, 6.23 mmol, 3.2 equiv) with triethylamine (869 mL, 6.23 mmol, 3.2 equiv) in dry THF, following the general procedure. The product was purified by recrystallization using a combination of DCM and MeOH, which gave the product as a white crystal in 89.0% yield (890 mg). ^{1}H NMR (500 MHz, $CDCl_3$) δ 8.09−8.12 (d, 3H) 7.87−7.89 (d, 3H), 7.66−7.71 (t, 3H), 7.43−7.48 (t, 3H), 5.31 (s, 6H), 1.13−1.18 (t, 3H), 0.91−0.99 (q, 2H); ^{13}C NMR (125 MHz, $CDCl_3$) δ 146.47, 136.58, 133.96, 127.91, 127.76, 124.70, 61.96, 6.40, 1.96; ^{29}Si NMR (59.6 MHz, $CDCl_3$) δ −42.11; HRMS (ESI/QTOF) m/z $[M + H]^+$ calculated for $C_{23}H_{23}N_3O_9Si$ 513.5340, found 513.1215.

*Tris(2-nitrobenzyloxy)phenylsilane (**TONBPS**).* To a solution of trichlorophenylsilane (284 mL, 1.78 mmol, 1 equiv) dissolved in dry THF was added dropwise to a mixture of 2-nitrobenzyl alcohol (873 mg, 5.7 mmol, 3.2 equiv) with triethylamine (794 mL, 5.7 mmol, 3.2 equiv) in dry THF, following the general procedure. The product was purified by recrystallization using a combination of DCM and MeOH, which yielded the product as a white crystal in 94.09% (940 mg). ^{1}H NMR (500 MHz, $CDCl_3$) δ 8.09−8.11 (d, 3H), 7.93−7.95 (d, 3H), 7.77−7.79 (d, 2H), 7.67−7.70 (t, 3H), 7.54−7.57 (t, 1H), 7.44−7.49 (m, 5H), 5.39 (s, 6H); ^{13}C NMR (125 MHz, $CDCl_3$) δ 146.43, 136.36, 134.70, 134.04, 131.53, 128.50, 127.98, 127.82, 124.75, 62.53; ^{29}Si NMR (59.6 MHz, $CDCl_3$) δ −56.11; HRMS (ESI/QTOF) m/z $[M + H]^+$ calculated for $C_{27}H_{23}N_3O_9Si$ 561.5780, found 561.1202.

Photochemical Properties/Polymerization. *Typical Reaction Conditions.* All photoreactions were conducted with a broad spectrum 450 W medium-pressure mercury lamp (250−400 nm lamp, 100 mw/cm^2 output measured at the sample) in a blackout cabinet. To prevent the degradation of silanes from the heat produced from the lamp, a cooling tube connected to a water-circulating chiller was used, as was an air circulation system exchanging air between inside and outside the cabinet. Samples were in NMR tubes and/or quartz cuvettes as needed. The distance between the light source and the samples was 20 cm.

*Procedure for Confirming **NsBAld** Formation as the Byproduct from **ONBTES** Photodecomposition.* A quartz cuvette containing a solution of **ONBTES** (0.55 M) in acetonitrile and water (4:1, following the patent procedure) was prepared and exposed to irradiation for 6 h. After that, a sample (420 μM) was prepared for UV−vis analysis, and the two were compared. $CDCl_3$ study: 7.8 mg of ONBTES (267.40 g/mol) was added to 10 mL of $CDCl_3$ along with 0.525 mL of DI water (1:1 equiv) resulting in a ∼2916 μM solution. This solution was diluted to 780 μM for UV−vis analysis. After the UV−vis was blanked with $CDCl_3$, 1 mL of the dilute solution was used to prime to the cuvette, and a second mL was used for analysis. Solutions were analyzed ambiently with UV 365 nm LED (Thor Laboratories, ∼25 mW/cm^2) over 1 h, with spectra taken every 5 min. Samples were vortexed prior to transfer for dilution and analysis.

*Procedure for Calculating the Molar Absorption Coefficient (e) for **ONBRSs**.* These coefficients were obtained by using the Beer−Lambert law after measuring the absorbance of

https://doi.org/10.1021/acsomega.4c04837
ACS Omega 2024, 9, 40650−40664

each **ONBRS** at 4 different concentrations in chloroform. The concentration versus absorption graph was plotted for each of them in order to determine the best-fit slope of the line at different absorption maxima. The obtained extinction coefficients were used to calculate the absorbances for all NMR samples. Therefore, these absorbances with initiated light intensity were used to calculate the moles of absorbed photons.

*Procedure for the Determination of the **ONBRS**'s Photoreaction Conditions.* NMR tubes containing solutions of each of the monofunctionalized **ONBRS** compounds (**ONBTES** and **ONBTPS**, both at a concentration of 0.55 M) in 0.7 mL of deuterated chloroform ($CDCl_3$), together with either water or **DBTDL**, were prepared and exposed to irradiation for a duration of 9 h. A total of 24 experiments were performed. Twelve trials were undertaken to assess the impact of varying quantities of water, particularly 1, 2, 3, 4, 5, and 6 equiv. Additionally, 12 trials were conducted to evaluate the influence of different percentages of catalyst, particularly 0, 5, 10, 15, 20, and 25 mol %. These solutions were prepared and kept in NMR tubes. To monitor the photocleavage, obtained ^{1}H NMR spectra were used at varied irradiation time intervals (10 time points). Using the benzyl methylene peak as a reference, we measured the decomposition percentage of **ONBRS**s by considering the ethyl/phenyl peaks as internal standards.

*Procedure for the Determination of the **ONBRS**'s Photophysical Properties and Characterizing the Photoproducts.* NMR tubes containing solutions of each of the **ONBRS** compounds (0.55 M) in 0.7 mL of chloroform-d_6 ($CDCl_3$) or acetonitrile-d_3 (CD_3CN, only for **ONBTES** and **BONBDES**), together with water (in different ratios depending on the number of **ONB** substituents) and 10 mol % **DBTDL**, were prepared and exposed to irradiation for 9 h (Tables 1 and S6). Following the previous procedure, the decomposition percentages of each sample after irradiation for 9 h were converted to product forming percentages, which were then converted to product moles for calculating the initial rate constant of the photodecomposition (k_{int}) and the quantum yields (Φ). The formed polymers were characterized using TGA, FTIR, and GPC (only for some of them).

*Procedure for **BONBDPS**'s Photopolymerization Using CH_3CN.* A quartz cuvette containing a solution of **BONBDPS** (0.55 M) in 0.7 mL of acetonitrile (CH_3CN), together with 2 equiv of water and 5 mol % of **DBTDL**, was prepared and exposed to irradiation for a duration of 24 h. GPC was used to characterize the formed polymer.

Surface Modification Using Trifunctionalized Derivatives of ONBRS. *Procedure for Coating TLC Using **TONBPS**.* A glass-backed TLC experiment was conducted, and it was partly masked with alphabet letters. Subsequently, it was immersed in a solution consisting of **TONBPS** (0.6560 g, 1 equiv), H_2O (3 equiv), and 10 mol % of **DBTDL** in 1.5 mL of THF (1.06 M). The system was exposed to irradiation for three hours. After the removal of the letters, TLC was rinsed with THF.

Etching Surfaces. Cleaning the surfaces of the glass plate and silicon wafer was accomplished by submerging them in acetone and then sonicating them for 10 min. Each sample was removed from acetone and submerged in a mixture of acetone:ethanol (1:1) and then sonicated for 10 min. After removing each sample and rinsing them with DI water, an acid solution containing H_2SO_4 and H_2O in a ratio of 7:3 was used to etch the samples' surfaces for 2 h, followed by rinsing both samples with DI water.

*Procedure for Coating Silicon Wafer and Glass Plate Using **TONBES**.* Each surface was partly covered with a foil. Subsequently, each was immersed separately in a solution consisting of **TONBES** (0.6560 g, 1 equiv), H_2O (3 equiv), and 10 mol % of **DBTDL** in 1.5 mL of THF (1.06 M). Both systems were exposed to irradiation for three hours. After removal of the foil, both surfaces were rinsed with THF.

■ ASSOCIATED CONTENT

Supporting Information

The Supporting Information is available free of charge at https://pubs.acs.org/doi/10.1021/acsomega.4c04837.

Supplementary figures, tables, materials, analytical methods, detailed synthesis procedures, and characterization (PDF)

X-ray crystal files (ZIP)

■ AUTHOR INFORMATION

Corresponding Author

Joseph C. Furgal − *Department of Chemistry and Center for Photochemical Sciences, Bowling Green State University, Bowling Green, Ohio 43403, United States;* orcid.org/0000-0002-7040-0793; Email: furgalj@bgsu.edu

Authors

Mahmud R. Rashed − *Department of Chemistry and Center for Photochemical Sciences, Bowling Green State University, Bowling Green, Ohio 43403, United States*

Cory B. Sims − *Department of Chemistry and Center for Photochemical Sciences, Bowling Green State University, Bowling Green, Ohio 43403, United States*

Shahrea Mahbub − *Department of Chemistry and Center for Photochemical Sciences, Bowling Green State University, Bowling Green, Ohio 43403, United States*

Nai-hsuan Hu − *Department of Chemistry and Center for Photochemical Sciences, Bowling Green State University, Bowling Green, Ohio 43403, United States*

Ashley N. Greene − *Department of Chemistry and Center for Photochemical Sciences, Bowling Green State University, Bowling Green, Ohio 43403, United States*

Herenia Espitia Armenta − *Department of Chemistry and Center for Photochemical Sciences, Bowling Green State University, Bowling Green, Ohio 43403, United States*

Ryan A. Iarussi − *Department of Chemistry and Center for Photochemical Sciences, Bowling Green State University, Bowling Green, Ohio 43403, United States*

Complete contact information is available at: https://pubs.acs.org/10.1021/acsomega.4c04837

Funding

Funding was provided by Bowling Green State University (BGSU) startup funds, a BGSU Building Strength Grant, and partial support from the US National Science Foundation DMR-2137672.

Notes

The authors declare no competing financial interest.

J.C.F. and M.R.R. have submitted a United States Patent Application (63/605,641) in December 2023 on some of the content of this manuscript.

■ ACKNOWLEDGMENTS

The authors thank Bowling Green State University for access and use of instrumentation, Startup Funding, and a 2020 Building Strength Grant. The authors would like to thank Dr. Angel Ugrinov of the North Dakota State University Department of Chemistry for conducting high-resolution mass spectroscopy analysis on these compounds and Keyence sales specialist Jordan Marich for the usage of the VHX-7000 digital microscope with the EA-300 attachment. Joseph C. Furgal and Mahmud R. Rashed express their gratitude to Andrew Deller, and undergraduate students Ethan Chandler, Cheyenne Morris, Connor Owen, and Christian Arnold for their contributions to this work.

■ ABBREVIATIONS

R:methyl, ethyl, or phenyl group; **ONB**:2-nitrobenzyl alcohol; **NsBAld**:2-nitrosobenzyl aldehyde; TEA:triethylamine; **ONBTES**:2-nitrobenzyloxytriethylsilane; **ONBTPS**:2-nitrobenzyloxytriphenylsilane; **BONBDES**:bis(-2-nitrobenzyloxy)-diethylsilane; **BONBDPS**:bis(2-nitrobenzyloxy)diphenylsilane; **BONBMPS**:bis(2-nitrobenzyloxy)methylphenylsilane; **TONBES**:tris(-2-nitrobenzyloxy)ethylsilane; **TONBPS**:tris(2-nitrobenzyloxy)phenylsilane; **DBTDL**:dibutyltindilaurate; lamp:450 W medium-pressure mercury lamp (250−400 nm); CY:ceramic yield; TBAF:tetrabutylammonium fluoride; RTV-siloxane:room temperature-vulcanizing-siloxane; TLC:thin layer chromatography; and SCA:static contact angle

■ REFERENCES

(1) Issa, A. A.; El-Azazy, M.; Luyt, A. S. Kinetics of Alkoxysilanes Hydrolysis: An Empirical Approach. *Sci. Rep.* **2019**, *9* (1), No. 17624.
(2) Hu, N. H.; Lenora, C. U.; May, T. A.; Hershberger, N. C.; Furgal, J. C. In Situ Formed Methyl- Co -(Bis-R) Silsesquioxane Based Polymer Networks with Solvent Controlled Pore Size Distributions and High Surface Areas. *Mater. Chem. Front.* **2020**, *4* (3), 851−861.
(3) Brinker, C. J.; Scherer, G. *Sol-Gel Science*, 1st ed.; Academic Press, Inc.: Boston, MA, 1991 DOI: 10.1016/b978-0-08-057103-4.50001-5.
(4) Arkles, B.; Steinmetz, J.; Zazyczny, J.; Mehta, P. Factors Contributing to the Stability of Alkoxysilanes in Aqueous Solution. *J. Adhes. Sci. Technol.* **1992**, *6*, 193.
(5) Wright, J. D.; Sommerdijk, N. A. J. M. *Sol-Gel Materials: Chemistry and Applications*; CRC press, 2000; Vol. *4*.
(6) Furgal, J. C.; Lenora, C. U. Green Routes to Silicon-Based Materials and Their Environmental Implications. *Phys. Sci. Rev.* **2020**, *5* (1), No. 20190024.
(7) Ciriminna, R.; Pagliaro, M. Open Challenges in Sol − Gel Science and Technology. *J. Sol−Gel Sci. Technol.* **2022**, *101*, 29.
(8) Hyde, J. F.; Curry, J. W. The Preparation of Tetra-t-Butoxysilane and Tri-t-Butoxyfluorosilane. *J. Am. Chem. Soc.* **1955**, *77* (11), 3140−3141.
(9) Hasegawa, I.; Sakka, S. Treatment of Tetraalkoxysilanes with Amberlyst 15 Cation-Exchange Resin in Presence of Hexamethyldisiloxane. *Bull. Chem. Soc. Jpn.* **1987**, *60* (12), 4313−4316.
(10) Martin, B. *Solvolysis Reactions of Alkoxysilicon Compounds*; University of Leicester, 1961.
(11) Issa, A. A.; Luyt, A. S. Kinetics of Alkoxysilanes and Organoalkoxysilanes Polymerization: A Review. *Polymers*. **2019**, *11* (3). 537.
(12) Indumathy, B.; Sathiyanathan, P.; Prasad, G.; Reza, M. S.; Prabu, A. A.; Kim, H. A Comprehensive Review on Processing, Development and Applications of Organofunctional Silanes and Silane-Based Hyperbranched Polymers. *Polymers* **2023**, *15* (11), 2517.
(13) Igarashi, M.; Matsumoto, T.; Sato, K.; Ando, W.; Shimada, S. Nonhydrolytic Synthesis of Silanols by the Hydrogenolysis of Benzyloxysilanes. *Chem. Lett.* **2014**, *43* (4), 429−431.
(14) Klán, P.; Šolomek, T.; Bochet, C. G.; Blanc, A.; Givens, R.; Rubina, M.; Popik, V.; Kostikov, A.; Wirz, J. Photoremovable Protecting Groups in Chemistry and Biology: Reaction Mechanisms and Efficacy. *Chem. Rev.* **2013**, *113* (1), 119−191.
(15) Slanina, T.; Shrestha, P.; Palao, E.; Kand, D.; Peterson, J. A.; Dutton, A. S.; Rubinstein, N.; Weinstain, R.; Winter, A. H.; Klán, P. In Search of the Perfect Photocage: Structure-Reactivity Relationships in Meso-Methyl BODIPY Photoremovable Protecting Groups. *J. Am. Chem. Soc.* **2017**, *139* (42), 15168−15175.
(16) Barltrop, J. A.; Schofield, P. Photosensitive Protecting Groups. *Tetrahedron Lett.* **1962**, *3*, 697−699.
(17) Wang, P.; Lu, W.; Devalankar, D. A.; Ding, Z. Structurally Simple Benzyl-Type Photolabile Protecting Groups for Direct Release of Alcohols and Carboxylic Acids. *Org. Lett.* **2015**, *17* (9), 2114−2117.
(18) O'Hagan, M. P.; Duan, Z.; Huang, F.; Laps, S.; Dong, J.; Xia, F.; Willner, I. Photocleavable Ortho-Nitrobenzyl-Protected DNA Architectures and Their Applications. *Chem. Rev.* **2023**, *123* (10), 6839−6887.
(19) Brook, M. A.; Balduzzi, S.; Mohamed, M.; Gottardo, C. The Photolytic and Hydrolytic Lability of Sisyl (Si(SiMe3)3) Ethers, an Alcohol Protecting Group. *Tetrahedron* **1999**, *55* (33), 10027−10040.
(20) Ding, X.; Wang, P. Using the 3-Diethylaminobenzyl Group as a Photocage in Aqueous Solution. *J. Org. Chem.* **2018**, *83* (14), 7459−7466.
(21) Lenci, W. M. H. F. *CRC Handbook of Organic Photochemistry and Photobiology*; CRC Press: Boca Raton, 2004.
(22) Lammertsma, K.; Bharatam, P. V. Keto ⇋ Enol, Imine ⇌ Enamine, and Nitro ⇌ a Ci -Nitro Tautomerism and Their Interrelationship in Substituted Nitroethylenes. Keto, Imine, Nitro, and Vinyl Substituent Effects and the Importance of H-Bonding. *J. Org. Chem.* **2000**, *65* (15), 4662−4670.
(23) Il'ichev, Y. V.; Schwörer, M. A.; Wirz, J. Photochemical Reaction Mechanisms of 2-Nitrobenzyl Compounds: Methyl Ethers and Caged ATP. *J. Am. Chem. Soc.* **2004**, *126* (14), 4581−4595.
(24) Hayase, S.; Onishi, Y. Photocurable Silicon Compound Composition. US4476290.1984.
(25) Hayase, S.; Onishi, Y.; Suzuki, S. Photo-Curable Epoxy Resin Composition. US4495042.1985.
(26) Yamamuro, T. Photodecomposing Organosilicon Compounds and Photopolymerizable Epoxy Resin Compositions Containing the Organosilicon Compounds. US4954534.1990.
(27) Hayase, S.; Yasunobu, O.; Suzuki, S.; Wada, M. Polymerization of epoxide with aluminum compound/organosilane catalyst. X. Photopolymerization of Epoxides with a New Catalyst Containing Photodecomposable Organosilane Compound and Electrical Properties of the Epoxy Resins Photocured. *Nippon Kagaku Kaishi* **1985**, *3*, 328−333.
(28) Suzuiki, S.; Wada, M.; Hayase, K. RESIN COMPOSITION. US4599155.1986.
(29) Jung, S.; Zafar, U.; Achary, L. S. K.; Koo, C. M. Ligand Chemistry for Surface Functionalization in MXenes: A Review. *EcoMat* **2023**, *5* (10), 1−33.
(30) Velleman, L.; Shearer, C. J.; Ellis, A. V.; Losic, D.; Voelcker, N. H.; Shapter, J. G. Fabrication of Self-Supporting Porous Silicon Membranes and Tuning Transport Properties by Surface Functionalization. *Nanoscale* **2010**, *2* (9), 1756.
(31) Rehman, S.; Khan, K.; Mujahid, M.; Nosheen, S. Synthesis of Nano-Hydroxyapatite and Its Rapid Mediated Surface Functionalization by Silane Coupling Agent. *Mater. Sci. Eng., C* **2016**, *58*, 675−681.
(32) Hicks, J. C.; Dabestani, R.; Buchanan, A. C.; Jones, C. W. Spacing and Site Isolation of Amine Groups in 3-Aminopropyl-Grafted Silica Materials: The Role of Protecting Groups. *Chem. Mater.* **2006**, *18* (21), 5022−5032.
(33) Álvarez, M.; Best, A.; Pradhan-Kadam, S.; Koynov, K.; Jonas, U.; Kreiter, M. Single-Photon and Two-Photon Induced Photo-

https://doi.org/10.1021/acsomega.4c04837
ACS Omega 2024, 9, 40650−40664

cleavage for Monolayers of an Alkyltriethoxysilane with a Photoprotected Carboxylic Ester. *Adv. Mater.* **2008**, *20* (23), 4563−4567.
(34) Jonas, U.; Del Campo, A.; Krüger, C.; Glasser, G.; Boos, D. Colloidal Assemblies on Patterned Silane Layers. *Proc. Natl. Acad. Sci. U.S.A.* **2002**, *99* (8), 5034−5039.
(35) Doshi, D. A.; Huesing, N. K.; Lu, M.; Fan, H.; Lu, Y.; Simmons-Potter, K.; Potter, J.; Hurd, A. J.; Brinker, C. J. Optically Defined Multifunctional Patterning of Photosensitive Thin-Film Silica Mesophases. *Science* **2000**, *290* (5489), 107−111.
(36) Yan, F.; Chen, L.; Tang, Q.; Wang, R. Synthesis and Characterization of a Photocleavable Cross-Linker and Its Application on Tunable Surface Modification and Protein Photodelivery. *Bioconjugate Chem.* **2004**, *15* (5), 1030−1036.
(37) Chen, D.; Ni, C.; Yang, C.; Li, Y.; Wen, X.; Frank, C. W.; Xie, T.; Ren, H.; Zhao, Q. Orthogonal Photochemistry toward Direct Encryption of a 3D-Printed Hydrogel. *Adv. Mater.* **2023**, *35* (14), No. 2209956.
(38) Ciriminna, R.; Pagliaro, M. Open Challenges in Sol−Gel Science and Technology. *J. Sol−Gel Sci. Technol.* **2022**, *101* (1), 29−36.
(39) Marciniec, B.; Dutkiewicz, M.; Maciejewski, H.; Kubicki, M. New, Effective Method of Synthesis and Structural Characterization of Octakis(3-Chloropropyl)Octasilsesquioxane. *Organometallics* **2008**, *27* (4), 793−794.
(40) van Der Weij, F. W. The Action of Tin Compounds in Condensation-type RTV Silicone Rubbers. *Die Makromol. Chem.* **1980**, *181* (12), 2541−2548.
(41) Ji, J.; Ge, X.; Pang, X.; Liu, R.; Wen, S.; Sun, J.; Liang, W.; Ge, J.; Chen, X. Synthesis and Characterization of Room Temperature Vulcanized Silicone Rubber Using Methoxyl-Capped MQ Silicone Resin as Self-Reinforced Cross-Linker. *Polymers.* **2019**, *11* (7). 1142.
(42) Speight, J. G. Redox Transformations. In *Reaction Mechanisms in Environmental Engineering*; Elsevier, 2018; pp 231−267. DOI: 10.1016/b978-0-12-804422-3.00007-9.
(43) Wu, X.; Fu, Q.; Kumar, D.; Ho, J. W. C.; Kanhere, P.; Zhou, H.; Chen, Z. Mechanically Robust Superhydrophobic and Superoleophobic Coatings Derived by Sol-Gel Method. *Mater. Des.* **2016**, *89*, 1302−1309.
(44) Dirè, S.; Tagliazucca, V.; Callone, E.; Quaranta, A. Effect of Functional Groups on Condensation and Properties of Sol-Gel Silica Nanoparticles Prepared by Direct Synthesis from Organoalkoxysilanes. *Mater. Chem. Phys.* **2011**, *126* (3), 909−917.
(45) De Ferri, L.; Lottici, P. P.; Lorenzi, A.; Montenero, A.; Salvioli-Mariani, E. Study of Silica Nanoparticles - Polysiloxane Hydrophobic Treatments for Stone-Based Monument Protection. *J. Cult. Heritage* **2011**, *12* (4), 356−363.
(46) Scott, T. F.; Kowalski, B.; Sullivan, A. C.; Bowman, C. N.; McLeod, R. R. Two-Color Single-Photon Photoinitiation and Photoinhibition for Subdiffraction Photolithography. *Science* **2009**, *324* (2009), 913−917.
(47) Berkowski, K. L.; Plunkett, K. N.; Yu, Q.; Moore, J. S. Introduction to Photolithography: Preparation of Microscale Polymer Silhouettes. *J. Chem. Educ.* **2005**, *82* (9), 1365−1369.
(48) Xi, W.; Peng, H.; Aguirre-Soto, A.; Kloxin, C. J.; Stansbury, J. W.; Bowman, C. N. Spatial and Temporal Control of Thiol-Michael Addition via Photocaged Superbase in Photopatterning and Two-Stage Polymer Networks Formation. *Macromolecules* **2014**, *47*, 6159.
(49) Sims, C. B.; Lenora, C. U.; Furgal, J. C. Hybrid Tri-Cure Organo-Silicon Coatings for Monument Preservation. *Coatings* **2022**, *12* (8), 1098. .

https://doi.org/10.1021/acsomega.4c04837
ACS Omega 2024, 9, 40650−40664